Journal of the Korean Nuclear Society
Volume 30, Number 3, pp.202~211, June 1998

A Study on the Improvement of Stress Field Analysis in a Domain Composed of Dissimilar Materials

Kee-Nam Song
Korea Atomic Energy Research Institute
150 Dukjin-dong, Yusong-gu, Taejon 305-353, Korea

Jin-Seok Lee
Korea Nuclear Fuel Company
150 Dukjin-dong, Yusong-gu, Taejon 305-353, Korea

(Received July 14, 1997)

Abstract

Interfacial stresses at two-material interfaces and initial displacement field over the entire domain are obtained by modifying the potential energy functional with a penalty function, which enforces continuity of the stresses at the interface of two materials. Based on the initial displacement field and interfacial stresses, a new methodology to generate a continuous stress field over the entire domain has been proposed by combining the modified projection method of stress-smoothing and Loubignac' s iterative method of improving the displacement field. Stress analysis is carried out on two examples made of dissimilar materials : one is a two-material cantilever composed of highly dissimilar materials and the other is a zirconium-lined cladding tube made of slightly dissimilar materials. Results of the analysis show that the proposed method provides an improved continuous stress field over the entire domain, and accurately predicts the nodal stresses at the interface, while the conventional displacement-based finite element method produces significant stress discontinuities at the interface. In addition, the total strain energy evaluated from the improved continuous stress field converges to the exact value in a few iterations.

1. Introduction

Media consisting of different materials are widely used in engineering structures. Examples include thermostats for measuring temperature, metallic parts in the etched silicon bases of microchips, attachments between prosthetic materials and biological tissues in orthopedic biomechanics, heat-resistant materials in aerospace vehicles and zirconium-lined cladding tubes of nuclear fuel rods. In such media, accurate evaluation of the stresses at the interfaces between dissimilar materials is usually of significant importance in both their analysis and design[1]. To ensure a perfect bond, the computed interfacial stresses should not exceed the bond strength, otherwise separation may occur, which could completely change the displacements and stresses, requiring re-analysis

with updated interface conditions.

Assuming a perfect bond at the interface, i.e., no separation or slip at the interface, the in-plane tangential strain must be continuous, while the normal and shear strains may be discontinuous [1,2]. The stress boundary conditions at the interface are determined from the required continuity of the traction vector. That is, in contrast to the strain components, the normal and shear stress components are required to be continuous, while the tangential component should be discontinuous.

In the displacement-based finite element method, the displacements are the primary unknowns of the analysis, and are usually taken to be continuous to the degree that the functional of the problem requires. The stresses in each element are then evaluated based on the displacements and the constitutive relations. However, such a consistent procedure results in stresses which are incompatible at the interface between adjacent elements. To overcome this shortcoming, several procedures have been suggested and proved to be effective in the analysis of homogeneous media because of small discrepancies of inter-element stresses in the literature[3-5] which are primarily of a post-processing nature, and are based on computed nodal displacements. The stress incompatibility, however, becomes evident, especially at a two-material interface. It is clear that, even between two dissimilar materials, the components of the stress tensor acting on the interface (i.e., normal and shear stresses) must be continuous. Therefore, the foregoing post-processing methods which could overcome a violation of the inter-element equilibrium are not suitable in the analysis of non-homogeneous media, even though mesh refinement is employed around the two-material interfaces. For, although mesh refinement could reduce the discrepancies of inter-element stresses, there still remains a problem to build the stress field, composed of both continuous and discontinuous stress components inherently.

Recently, research to find only accurate stress fields at two material interfaces has been carried out. Shirazi-Adl[1,2] proposed that a penalty function be added to the usual potential energy functional. The penalty function enforces the compatibility of tractions on the element interfaces. The modified functional is minimized and the equations generated are solved in the conventional manner. The stresses are then calculated from the predicted nodal displacements using strain-displacement relations and constitutive equations. This formulation results in no extra degrees of freedom but the structural band-width may increase. Chouchaoui and Shirazi-Adl[6] and Kim[7] proposed mixed variational formulations based on the Hellinger-Reissner theorem and Kim[8] proposed a perturbed Lagrangian method for the 2-D dissimilar bonding problem.

In this study, we combine a penalty method and a post-processing method which build new displacement fields and displacement-consistent stress fields iteratively. A procedure to predict an accurate and continuous stress field both at the interface and over the entire domain is thus proposed.

2. Finite Element Formulation

Figure 1 shows the domain consisting of dissimilar materials. Assuming a perfect bond at a two-material interface, the constraint equations on the interface tractions may be written as[1,2] :

$$T_i^a + T_i^b = 0 \tag{1}$$

where superscripts a and b denote material sides of the interface and subscript i varies from 1 to 3 in a three-dimensional analysis. This equation can

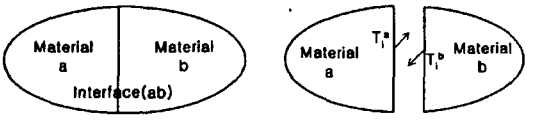

Fig. 1. Interface Traction Acting on a Bi-metallic Interface Between Two Regions a and b.

be regarded as the Euler equation of the conventional potential energy functional. The usual potential energy, π_p, may be modified by imposing the constraint equation (1) by a penalty function procedure as :

$$\pi_p^* = \pi_p + \frac{1}{2}\alpha \int_S (T_i^a + T_i^b)^2 \, dS \tag{2}$$

where $[n]$ is a penalty number and S is the common interface surface. The first term on the right-hand side results in well-known element equations and is not discussed further. In the second penalty term, T_i^a and T_i^b may be expressed as vectors by :

$$\{T^a\} = [n^a]\,[E^a]\,[B^a]\,\{d^a\} \tag{3}$$

$$\{T^b\} = [n^b]\,[E^b]\,[B^b]\,\{d^b\} \tag{4}$$

where $[n]$ is the matrix of the directional cosines of the unit outward vector normal to the interface S, $[E]$ the elasticity matrix, $[B]$ the strain-displacement matrix, and {d} the column vector of the element nodal displacements. Combining the two adjacent interface elements into one with $\{d^{ab}\}$ as the column vector of displacements, we obtain :

$$\{T^a + T^b\} = [K^{ab}]\{d^{ab}\} \tag{5}$$

where

$$[K^{ab}] = [n^a]\,([E^a]\,[B^a]\,[T^a] - [E^b][B^b][T^b]) \tag{6}$$

and $[T_a]$ and $[T_b]$ are the transformation matrices.

Finally, the symmetric stiffness matrix for a two-material interface due to the penalty function is :

$$[K_p] = \int_S [K^{ab}]^T [K^{ab}] dS \tag{7}$$

which should be added to the conventional stiffness matrix, $[K]$

$$\text{i.e., } [K^*] = [K] + \alpha\,[K_p] \tag{8}$$

Then, the system equations become :

$$[K^*]\,\{u\} = \{f\} \tag{9}$$

where $\{u\}$ is a column vector of nodal displacement components for the entire domain : $\{f\}$ is the column vector of the resultant nodal forces.

The terms in the interface penalty matrix $[K_p]$ are noted to be larger than those in the conventional stiffness matrix, the difference being of the same order as that of the moduli. Considering the difference of the order of the moduli, therefore, an appropriate penalty number could be selected in the formulation. In general, through analysis using some different values of the penalty number, an appropriate penalty number, which does not significantly affect the results, is selected.

3. Build-up of the Continuous Generalized-stress Field

Assuming that the generalized-stress field (i.e., the field composed of continuous stress/strain components at the interface) maintains C° continuity, the generalized-stress field,$\{\sigma^*\}$, is expressed as a linear combination of the nodal stress vector, $\{\overline{\sigma}^*\}$, and the shape function vector, $[N^*]$, as follows :

$$\{\sigma^*\} = [N^*]\{\overline{\sigma}^*\} \tag{10}$$

Usually in the analysis of homogeneous media, the nodal stress vector, $\{\overline{\sigma}^*\}$, can be obtained by the following projection method[9] of discontinuous stress field, $\{\overline{\sigma}^*\}$, from the conventional finite element method in the mean sense :

$$I = \int_{\Omega} [N^*]^T(\{\sigma^*\}-\{\sigma\})d\Omega = 0 \qquad (11)$$

At the two-material interface, however, the generalized stress field should be the same as the interface tractions, $\{\sigma_{sp}\}$, which are obtained from the finite element formulation of Sec. 2.

$$\{\sigma^*\} = \{\sigma_{sp}\} \qquad (12)$$

For the generalized-stress field to satisfy the interface tractions, imposing the specified tractions of Eq. (12) may modify Eq. (11) of a penalty function as follows :

$$I^* = I + \alpha_\sigma \int_S [N^*]^T(\{\sigma^*\}-\{\sigma_{sp}\})dS = 0 \qquad (13)$$

where α_σ is a penalty number and S is the common interface surface. Re-arranging Eq.(13) with respect to $\{\overline{\sigma}^*\}$ yields the following :

$$\{\overline{\sigma}^*\}\left(\int_{\Omega} [N^*]^T [N^*]d\Omega + \alpha_\sigma \int_S [N^*]^T [N^*]dS\right)$$

$$= \int_{\Omega} [N^*]^T\{\sigma\}d\Omega + \alpha_\sigma \int_S [N^*]^T\{\sigma_{sp}\}dS \qquad (14)$$

Solving Eq. (14) for $\{\overline{\sigma}^*\}$, the continuous generalized-stress field satisfying the specified tractions at the two-material interface is obtained from Eq. (10).

4. Iterative Method

Nodal force vector, $\{f^*\}$, due to a continuous generalized-stress field, $\{\sigma^*\}$, is obtained by the following equilibrium equations :

$$\int_{\Omega} [B]^{*T}\{\sigma^*\}d\Omega = \{f^*\} \qquad (15)$$

where $[B]^*$ denotes a generalized strain-displacement matrix defined as follows :
$[B]^* = [B]$ for continuous stress components, and
$[B]^* = [E][B]$ for continuous strain components.

Since the nodal force vector, $\{f^*\}$, does not equal the force, $\{f\}$, from the original finite element equilibrium, the following iterative algorithm builds a new displacement field. While Loubignac *et al.*[10] used simple nodal averaging to obtain $\{\sigma^*\}$ which could be inaccurate at the two-material interface, a continuous stress field obtained from the procedure in Sec. 3 is used.

i) $\{\triangle u\}^i = [K]^{-1}(\{f\} - \sum_{element} \int_{\Omega_e} [B]^{*T}\{\sigma^*\}^i d\Omega_e)$ (16)

ii) Compute the nodal force vector that corresponds to the stress, σ^*

$$f_e = \int_{\Omega_e} [B]^T \sigma^* d\Omega_e = \int_{\Omega_e} [B]^T N_i^* \, d\Omega_e \, S^i \qquad (17)$$

$$f^* = \sum_{element} f_e = \sum_{element} \int_{\Omega_e} [B]^T \sigma^* d\Omega_e$$

$$= \sum_{element} \int_{\Omega e} [B]^T N_i^* d\Omega_e \, S^i \qquad (18)$$

The L^2-norm of force-imbalance, $\| \Delta f \|_i$ and ratio of L^2-norm of force-imbalance, R_i, at the *i-th* iteration is defined as follows :

$$\| \Delta f \|_i^2 \equiv \int_{\Omega} (f-f^*)^T (f-f^*)d\Omega \qquad (19)$$

$$R_i \equiv \frac{\| \Delta f \|_i}{\| \Delta f \|_0} \qquad (20)$$

iii) $\{u\}^{i+1} = \{u\}^i + \{\triangle u\}^i$, $i = 1, 2, 3\cdots$ (21)

iv) $\{\sigma\}^{i+1} = [E][B]^* \{u\}^{i+1}$ (22)

v) Build a new continuous stress field using the procedure in Sec. 3.

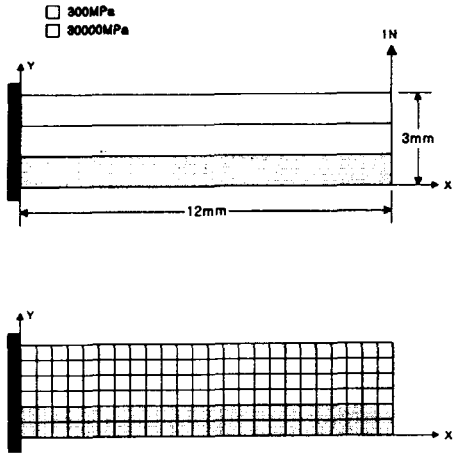

Fig. 2. A Two-material Cantilever Beam Under End Load.

vi) Go to step i) unless the L^2-norm of the perturbed displacement, $\| \Delta u \|'$ is less than a preset value.

The total strain energy (U_{total}) expression is defined as :

$$U_{total} = \frac{1}{2}\int_V \sigma^{*T} \varepsilon^* dV = \frac{1}{2}\int_V \sigma^* E^{-1} \sigma^* dV \quad (23)$$

where ε^* denotes the strain in the domain.

5. Numerical Examples

5.1. Example 1 : Two-material Cantilever Beam Under End Load

Figure 2 shows a cantilever beam composed of two materials with a 100 times difference in elastic moduli (Young's moduli) and shows its finite element model with quadrilateral plane stress elements. The end forces are computed and applied in a manner consistent with the quadratic variation of end shear stresses in each material region evaluated based on the analytical solution[12]. The results for the penalty

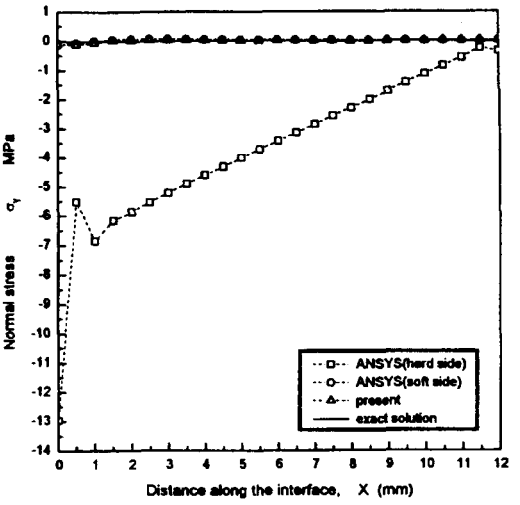

Fig. 3. Nodal Normal Stress on the Two-material Interface.

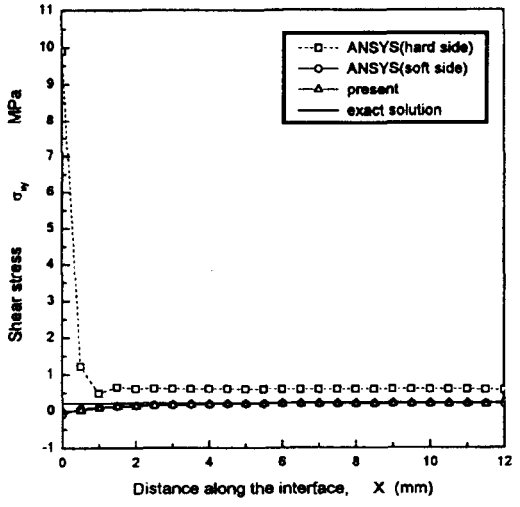

Fig. 4. Nodal Shear Stress on the Two-material Interface.

formulation are based on $\alpha = 0$, $\alpha_s = 10000$ and one-point integration. The analytical solution is compared to the conventional finite element solution of the ANSYS finite element code[11] and the present results. The variation of the stresses at the two-material interface along the beam is

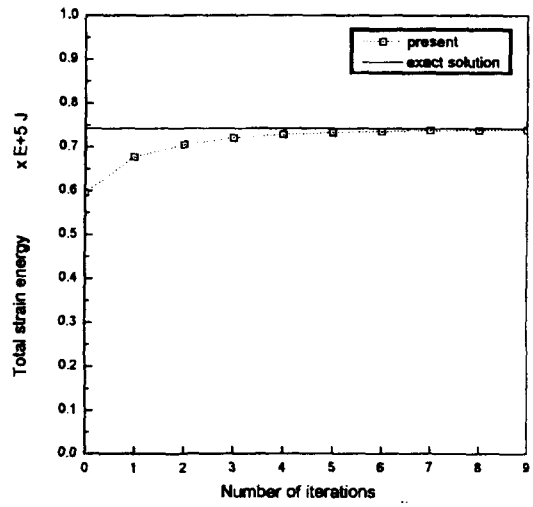

Fig. 5. Total Strain Energy vs. Iteration Numbers for the Two-material Cantilever Beam Under End Shear.

shown in Figs. 3 and 4. Comparison of the results of the conventional finite element analysis reveals a very significant discontinuity between the computed stresses on the hard and soft sides of the interface. However, the present method yields identical stresses in both materials at the interface. In addition, both stresses from the present method and the conventional finite element stresses on the soft side of the interface are in agreement with the exact results (σ_y = 0, τ_{xy} = 0.219298 MPa)[12] everywhere except in the region close to the fixed end. The variation in the total strain energy calculated from Eq. (22) as iteration numbers as shown in Fig. 5. The total strain energy at the 0-*th* iteration denotes a value from the conventional average stress field. Figure 5 shows that the total strain energy rapidly increases and converges to the analytical solution (U_{total} = 0.74210E-1 MJ) in a few iterations. When the moduli are reversed, similar observations as in this example are made[13].

From Figs. 3 and 4, the stresses on the soft side of the two-material interface seem to be more reliable than the harder one. However, we can see that this observation is not general in the following example.

5.2. Example 2 : Thick-walled Cylinder Subjected to Internal and External Pressure

Figure 6 shows a finite element model of a nuclear fuel rod cladding tube subjected to uniform internal and external pressure. The specified pressure values in Fig. 6 represent the fuel rod' s internal pressure and the system pressure at the pressurized water nuclear reactor' s cold condition, respectively. Since the wall thickness exceeds the inner radius by more than approximately 10%, the cladding tube is considered to be a thick-walled cylinder[14]. Two kinds of stress analysis for the finite element model shown in Fig. 6 have been carried out, with the plane strain conditions.

First, stress analysis on the fuel rod cladding tube of isotropic Zircaloy-4 material ($E_1 = E_2$ = 1.0515E+05N/mm^2, $\nu_1 = \nu_2$ = 0.35)[15] was carried out to assure the validity of the present method, combining the conjugate approximations for the stress-smoothing and Loubignac' s iterative method for the improved displacement field. Variations of the ratio of the L^2-norm of force-imbalance as iteration numbers are shown in Fig. 7. The value of the function at iteration number 0 in Fig. 7 denotes the ratio of the L^2-norm of force-imbalance, based on the stress field generated from the conventional displacement-based finite element codes, such as ANSYS. The ratio of the L^2-norm of force-imbalance rapidly decreases and monotonously converges into some value, which means that the stress field generated from combining the conjugate approximations and Loubignac' s iterative method is improving, satisfying the original finite element equilibrium equations. Variations of the total strain energy

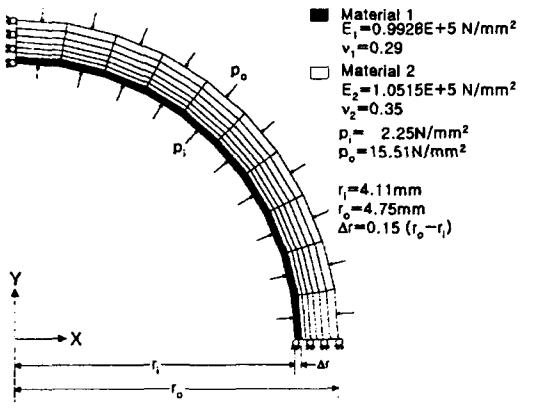

Fig. 6. Finite Element Model of a Fuel Rod Cladding Tube(Thick-walled Cylinder) Composed of Dissimilar Materials.

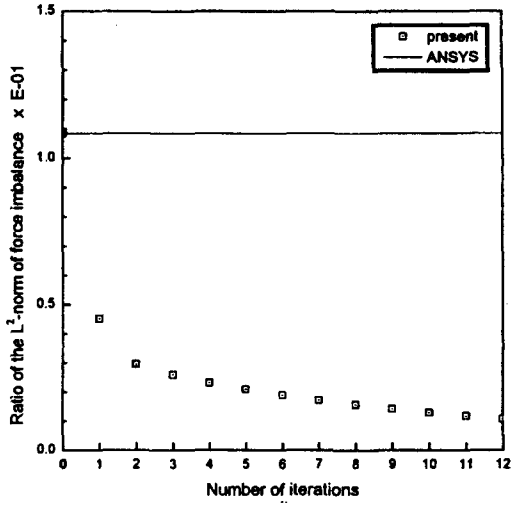

Fig. 7. Ratio of the L^2-Norm of Force Imbalance vs. Number of Iterations for the Isotropic Thick-walled Cylinder Model.

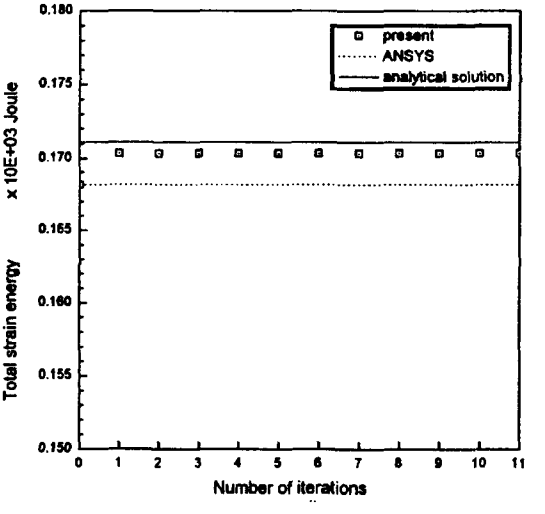

Fig. 8. Total Strain Energy vs. Iteration Numbers for the Isotropic Thick-walled Cylinder Model.

calculated from Eq. (22) as iteration numbers are shown in Fig. 8, where also the total strain energy from the finite element model shown in Fig. 6 and the exact solution (U_{total} = 0.17108E+03 Joule) [16] have been compared. Figure 8 shows that the total strain energy from present method rapidly increases and monotonously convergent at some value a little smaller than the exact solution in a few iterations.

Second, stress analysis on a fuel rod cladding tube composed of dissimilar materials, as shown in Fig. 6, has been carried out. The boiling water nuclear reactor' s zirconium-lined cladding tube, whose inner part, lined with pure zirconium, is softer than the outer part of the cladding tube, made of Zircaloy-2, is developed to resist stress-induced corrosion cracking. Interfacial stresses at the two-material interface and the continuous stress field over an entire domain are obtained from the procedures of Sec. 2, 3, and 4 in this study. Table 1 presents some of the results of the finite element analysis and compares them with those obtained by the analytical solution[16]. Once again, the discontinuity of radial stress at the two-material interface is strikingly large in the conventional displacement-based finite element method. The present study predicts continuous stresses which are close to the exact solution. Table 1 lists also the results for the hoop stress and radial stress, and the displacement at the two-material interface. Table 1 shows that the radial stress on the soft side of the two-material interface, as well as that on the harder side, is not

Table 1. Results for the Zirconium-lined Cladding Tube at the Two-material Interface

		Exact	Finite Element Method	
			Conventional	Present
stress (MPa)	σ_r^1 *	−4.4262	−3.6192	−4.5764
	σ_r^2	−4.4262	−5.7906	−4.5764
	σ_θ^1	−96.519	−96.475	−96.430
	σ_θ^2	−107.084	−107.059	−106.999
strain(x E−03)	ε_r^1	0.32286	0.33014	0.32114
	ε_r^2	0.44425	0.43275	0.44262
displacement at r=4.206mm (mm)	U_r^1 (= U_r^2)	−0.3675E−2	−0.3669E−2	−0.3699E−2

* Superscripts 1 and 2 denote the inner and outer sides of the two-material interface, respectively.

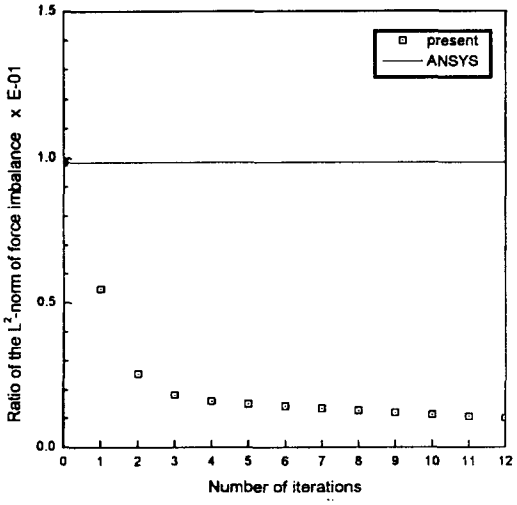

Fig. 9. Ratio of the L^2-Norm of Force Imbalance vs. Number of Iterations for the Thick-walled Cylinder Composed of Dissimilar Materials.

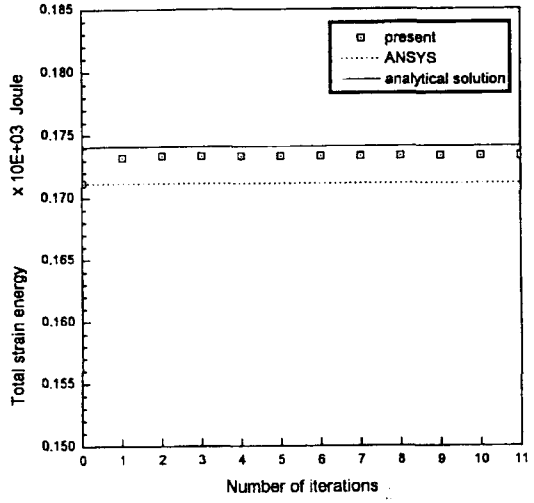

Fig. 10. Total Strain Energy vs. Iteration Numbers for the Thick-walled Cylinder Composed of Dissimilar Materials.

close to the exact solution. For the stresses at the two-material interface, therefore, the indication that stresses on the softer side of the two-material interface are more reliable than those on the harder side is not a general one. The results for the penalty formulation are based on $\alpha = \alpha_s = 10000$ and one-point integration. The variation of the ratio of the L^2-norm of force-imbalance and the variation of the total strain energy calculated from Eq. (22) as iteration numbers are shown in Figs. 9 and 10, respectively. Figure 9 shows that the ratio of the L^2-norm of force-imbalance is monotonously decreasing, which means that the stress field from present method is improved, satisfying the original finite element equilibrium equation. Figure 10 shows that the total strain energy from the present method is rapidly and monotonously convergent at some value a little

smaller than the exact solution (U_{total} = 0.17411E + 03 Joule) in a few iterations. This denotes that a more accurate stress field than that determined by the conventional finite element method could be obtained without too much computational cost.

7. Conclusions

An iterative procedure to calculate a continuous stress field over the entire domain, including the interface of dissimilar materials, is proposed by combining the modified projection method for stress-smoothing and Loubignac' s iterative method for the build-up of new displacement fields which satisfy finite element equilibrium equations. The initial displacement field and interfacial stresses are obtained by modifying the potential energy functional with a penalty function, which enforces the continuity of stresses at two-material interfaces. The proposed iterative procedure is used for stress analysis on two examples consisting of dissimilar materials and the results are compared with the exact solutions and those obtained from conventional finite element analysis. The proposed iterative procedure is performed satisfactorily in the test examples and is therefore considered to be a reliable method to generate a continuous stress field in the entire domain, including the interface of dissimilar materials. In contrast, the usual finite element formulation results in significantly discontinuous stresses at two-material interfaces.

References

1. A. Shirazi-Adl, "Finite element stress analysis of a push-out test Part 1 : Fixed interface using stress compatible elements," *ASME Journal of Biomechanical Engineering*, Vol.114, p111-118 (1992).
2. A. Shirazi-Adl, "An interface continuous stress penalty formulation for the finite element analysis of composite media," *Computers & Structures*, Vol.33, No.4, p951-956 (1989).
3. H. J. Brauchli and J. T. Oden, "Conjugate approximation function in finite-element analysis," *Quarterly of Applied Mathematics*, No.1, April, p65-90 (1971).
4. E. Hinton and J. S. Campbell, "Local and global smoothing of discontinuous finite element functions using a least squares method," *International Journal for Numerical Methods in Engineering*, Vol.8, p461-480 (1974).
5. O. C. Zienkiewicz and J. Z. Zhu, "The superconvergent patch recovery and *a posteriori* error estimates. Part 1 : The recovery technique," *International Journal for Numerical Methods in Engineering*, Vol. 33, p1331-1364 (1992).
6. B. Chouchaoui and A. Shirazi-Adl, " A mixed finite element formulation for the stress analysis of composite structures," *Computers & Structures*, Vol.43, No.4, p687-698 (1992).
7. D. S. Kim, *Finite element analysis of bonding problems based on a new mixed variational principle*, Ph.D. Thesis, KAIST (1994).
8. Y. H. Kim, *Analysis of 2-D bonding problems using perturbed Lagrangian method*, M.S. Thesis, KAIST (1994).
9. O. C. Zienkiewicz, Li Xi-Kui and S. Nakazawa, "Iterative solution of mixed problems and the stress recovery procedures," *Communications in Applied Numerical Method*, Vol.1, p3-9 (1985).
10. G. Loubignac, G. Cantin and G. Touzot, "Continuous stress field in finite element analysis," *AIAA Journal*, Vol.15, No.11, p1645-1646 (1977).
11. ANSYS User' s Manual for Revision 5.0, 1992, Swanson Analysis System, Inc.
12. N. I. Muskhelishvili, *Some basic problems of*

mathematical theory of Elasticity (Translated by J. R. M. Radok), p641-649, Noordhoff, Groningen, Holland (1963).

13. K-N. Song, "A Study on the interfacial stresses in the domain composed of highly dissimilar materials," *Proceedings of the KNS Spring Meeting*, Vol. II, p30-35 (1997).
14. A. C. Ugural and S. K. Fenster, *Advanced strength and applied elasticity : The SI version*, Elsevier North Holland, New York (1981).
15. "Zircadyne Properties & Applications," TWCA-8103-ZR, Teledyne Wahchang Albany, June (1984).
16. S. H. Crandall and N. C. Dahl, *An introduction to the mechanics of solids*, 2nd ed., McGraw-Hill Kogakusha, Tokyo (1978).